HHS Public Access

Author manuscript

Nat Neurosci. Author manuscript; available in PMC 2011 December 01.

Published in final edited form as:

Nat Neurosci. 2011 June ; 14(6): 727–735. doi:10.1038/nn.2804.

Mechanism of CaMKII regulation of AMPA receptor gating

Anders S. Kristensen[1,2], **Meagan A. Jenkins**[1], **Tue G. Banke**[1], **Arne Schousboe**[3], **Yuichi Makino**[4], **Richard C. Johnson**[4], **Richard Huganir**[4], and **Stephen F. Traynelis**[1]

[1] Department of Pharmacology, Emory University School of Medicine, Atlanta, Georgia 30322, USA

[2] Department of Medicinal Chemistry, University of Copenhagen, Copenhagen, DK2100, Denmark

[3] Department Pharmacology and Pharmacotherapy, University of Copenhagen, Copenhagen, DK2100, Denmark

[4] Department of Neuroscience and Howard Hughes Medical Institute, Johns Hopkins University School of Medicine, Baltimore, Maryland, USA

Abstract

The function, trafficking and synaptic signalling of AMPA receptors are tightly regulated by phosphorylation. CaMKII phosphorylates the GluA1 AMPA subunit at Ser831 to increase single channel conductance. We show for the first time that CaMKII increases the conductance of native heteromeric AMPA receptors in mouse hippocampal neurons via phosphorylation of Ser831. In addition, co-expression of TARPs with recombinant receptors is required for phosphoSer831 to increase conductance of heteromeric GluA1/GluA2 receptors. Finally, phosphorylation of Ser831 increases the efficiency with which each subunit can activate, independent of agonist efficacy, thereby increasing the likelihood that more receptor subunits will be simultaneously activated during gating. This underlies the observation that phosphoSer831 increases the frequency of openings to larger conductance levels rather than altering unitary conductance. Together, these findings suggest that CaMKII phosphorylation of GluA1-Ser831 decreases the activation energy for an intrasubunit conformational change that regulates the conductance of the receptor when the channel pore opens.

Keywords

AMPA receptor; GluA1; GluR1; CaMKII; LTP; channel gating; phosphorylation

Correspondence should be addressed to Stephen F. Traynelis (strayne@emory.edu).

Author contributions: ASK and MAJ performed patch clamp recordings from recombinant and neuronal receptors; MAJ performed all recordings with neurons from transgenic animals. TGB performed a subset of rapid agonist application experiments onto recombinant receptors. YM, RCJ, RH generated knock-in mice for this study. TGB and AS performed Xenopus oocyte recordings. SFT assisted with experimental design, participated in data analysis and interpretation. All authors contributed to writing of the manuscript.

INTRODUCTION

AMPA-selective glutamate receptors are ligand-gated cation channels that mediate fast excitatory neurotransmission in the brain, and thus play a role in many aspects of brain function including cognition, movement, learning, and memory[1]. The function and number of postsynaptic AMPA receptors is dynamically regulated by phosphorylation to control synaptic strength, a key feature of cellular models of learning and memory[2].

AMPA receptors are tetrameric assemblies of four subunits (GluA1-4), each containing two semiautonomous extracellular domains, an amino terminal domain and an agonist-binding domain. The agonist binding domain is linked to three membrane-spanning α-helices and a pore-forming re-entrant loop[1, 3]. The crystal structure of a homomeric GluA2 receptor in an antagonist-bound state shows that the extracellular domain posseses approximate 2-fold symmetry, while the ion channel pore-forming domains are arranged with 4-fold symmetry[3]. Each subunit has an intracellular C-terminal segment downstream of the third membrane spanning helix, and contains phosphorylation sites that regulate receptor gating, trafficking, and localization[4–8].

Cellular models of synaptic plasticity, such as long-term potentiation (LTP), are characterized by an AMPA receptor-dependent increase in excitatory post-synaptic current (EPSC) amplitude at hippocampal CA1 pyramidal cells[9]. This results either from enhanced AMPA receptor function or an increased delivery of AMPA receptors to the synapse[2, 6, 9, 10], although the relative contribution of these mechanisms to LTP is not fully understood. In addition, both the AMPA receptor GluA1 subunit and Ca^{2+}/calmodulin-dependent kinase II (CaMKII), a serine-threonine protein kinase highly expressed at excitatory synapses, are required for expression of LTP at mature hippocampal CA1 pyramidal cells[11–16]. Biochemical studies have identified a CaMKII phosphorylation site at Ser831 on the C-terminal domain of the GluA1 subunit[5, 17, 18]. Whereas GluA1-Ser831 phosphorylation does not appear to increase synaptic localization of GluA1-containing receptors[19], it does increase conductance of homomeric GluA1 receptors expressed in recombinant systems[4]. This potentiation is similar to the increased conductance of native AMPA receptors observed following LTP[4, 10, 20–22].

Here, we investigate the mechanism by which phosphorylation of native and recombinant GluA1-Ser831 increases AMPA receptor conductance. AMPA receptors exist in multiple open states with distinct conductance levels determined by agonist binding and the gating of individual subunits[23–27]. The AMPA receptor single channel conductance is a function of the number of agonist-bound subunits per receptor complex that are activated at any given moment[23–27]. Our data support previous work showing that phosphorylation of GluA1-Ser831 does not change individual conductance level amplitudes, but rather increases the relative occupation of larger conductance levels[4]. We show here that CaMKII increases conductance of both recombinant and native AMPA receptors via phosphorylation at GluA1-Ser831. A phosphomimic mutation in GluA1 enhances heteromeric GluA1/GluA2 receptor conductance when the transmembrane AMPA receptor regulatory proteins (TARPs) stargazin or γ8 are present. Finally, phosphorylation of GluA1 at Ser831 can increase the efficiency by which each subunit translates ligand-induced conformational changes within

the agonist binding domain to channel activation. We thus propose that CaMKII enhances gating of individual subunits in GluA1-containing AMPA receptors to increase the single channel conductance.

RESULTS

Control of neuronal AMPA receptor function by CaMKII

CaMKII phosphorylation of GluA1 enhances the single channel conductance of recombinant homomeric receptors[4]. Previous work has identified residue Ser831 in the GluA1 subunit as the primary site for CaMKII phosphorylation[5, 13, 17, 18] (Fig. 1a). We examined whether purified CaMKII affects the weighted mean conductance (γ_{MEAN}) of native hippocampal AMPA receptors, which express GluA1, GluA2, and GluA3 subunits[28]. Given the multiple AMPA receptor subunits expressed in hippocampal neurons, we assumed that AMPA receptors in outside-out patches possessed heterogeneous subunit compositions. Macroscopic currents, induced by bath application of 1 mM glutamate to outside-out patches isolated from cultured hippocampal neurons (Fig. 1b), were recorded either with or without purified CaMKII (2 U/ml) in the patch pipette (plus 0.1 μM Ca^{2+} and 10 μg/ml calmodulin). DL-AP5 (100 μM) and Mg^{2+} (1 mM) were added to the external solution to reduce the contribution of NMDA receptor activation, and cyclothiazide (100 μM) was added to reduce desensitization. A current response with a graded waveform (Fig. 1a–b) was generated by slowly washing glutamate from the bath. The γ_{MEAN} of AMPA receptors in the patch can be estimated using variance analysis of the current response during washout of agonist[26, 29] (Fig. 1b–c). Inclusion of purified CaMKII, Ca^{2+} and calmodulin in the patch pipette significantly increased the γ_{MEAN} from 4.3 ± 0.4 pS (n = 11; Fig. 1d) to 9.3 ± 0.4 pS (n = 12; $p < 0.001$; student's t-test; Fig. 1d). These results show that CaMKII controls the conductance of native hippocampal AMPA receptors, consistent with previous observations on recombinant homomeric GluA1 receptors[4, 30]. The reduced conductance observed in neurons compared to homomeric GluA1 (Fig. 1, Table 1) suggests inclusion of edited GluA2 subunits, which lowers unitary conductance when co-assembled with GluA1. The presence of GluA2-containing AMPA receptors is also consistent with the linear IV relationship [31] (Fig. 1a).

TARPs associate with AMPA receptors to control receptor trafficking and function[7]. CaMKII phosphorylation of a specific TARP, stargazin, appears to influence both trafficking of AMPA receptors as well as LTP of hippocampal synapses[32]. It was therefore necessary to determine whether the effects we observed in hippocampal neurons resulted directly from CaMKII phosphorylation of GluA1-Ser831 or indirectly via phosphorylation of associated proteins such as stargazin. To do this, we measured γ_{MEAN} in hippocampal neurons cultured from phosphodeficient gene knock-in mice expressing an alanine at the Ser831 phosphorylation site (GluA1-S831A) or alanine substitutions at both Ser831 and Ser845 (GluA1-S831A,S845A)[12, 16]. Inclusion of CaMKII, Ca^{2+} and calmodulin in the patch pipette did not increase the γ_{MEAN} of AMPA receptors from neurons expressing GluA1-S831A,S845A (4.7 ± 0.7 pS; n = 9) compared to control recordings obtained with Ca^{2+} and calmodulin alone (5.0 ± 0.8 pS; n = 11; p = 0.75; Fig. 1d). CaMKII similarly failed to increase γ_{MEAN} in neurons expressing GluA1-S831A (4.4 ± 0.5 pS; n = 15) compared to

control (p = 0.54). Introduction of the phosphomimic aspartate in place of GluA1-Ser831 and Ser845 (GluA1-S831D,S845D, Supplemental Fig. S1) significantly increased AMPA receptor γ_{MEAN} (8.4 ± 1.1 pS; n = 12) compared to GluA1-S831A,S845A and GluA1-S831A (p < 0.001, Fig. 1d). Moreover, the conductance of these phosphomimic mutant native AMPA receptors was not further increased by CaMKII (8.2 ± 1.4 pS; n = 8; p = 0.90; Fig. 1d). These data show that the increase in unitary conductance, $\gamma_{MEAN,}$ by CaMKII in native receptors reflects phosphorylation of GluA1-Ser831, and is not an indirect result of phosphorylation of other GluA1 residues or associated regulatory proteins.

Control of recombinant AMPA receptor function by CaMKII

We next explored the mechanistic basis for the CaMKII-dependent increase in γ_{MEAN}. We first tested whether potentiation of the AMPA receptor response by purified CaMKII could be fully accounted for by an increase in conductance. We recorded the current response to 1 mM glutamate from *Xenopus laevis* oocytes expressing homomeric GluA1-flip receptors (hereafter, GluA1), without coexpression of TARPs, using two electrode voltage-clamp both before and after injection of purified CaMKII (20 ng/μl) directly into the oocytes. CaMKII injection significantly potentiated the current response to 183 ± 15% of control (n = 13, p < 0.001, unpaired t-test) compared to buffer-injected oocytes (102 ± 3% of control; n = 5). We subsequently used a rapid perfusion system to apply a maximally effective concentration (10 mM) of glutamate onto excised outside-out patches from HEK cells transiently transfected with GluA1 (Supplemental Fig S2). Inclusion of purified CaMKII in the recording pipette increased the γ_{MEAN} determined using non-stationary variance analysis to 175 ± 15% of control (n = 9; p < 0.002; paired t-test), an almost identical increase when compared to that observed from injection of CaMKII directly into oocytes expressing GluA1 (Table 1). Identical results were found with stationary variance analysis (Table 1). However, CaMKII had no significant effect on γ_{MEAN} when a non-hydrolysable analogue of ATP (4 mM AMP-PNP) was included in the patch pipette (data not shown; p > 0.05; n = 3). Furthermore, CaMKII had no significant effect on γ_{MEAN} of GluA1-S831A, confirming previous findings that the effects of CaMKII on GluA1 reflected actions at Ser831[5, 17, 18] (Table 1). In addition, inclusion of CaMKII in the patch pipette did not change the GluA1 response rise time (10–90% rise time 0.55 ± 0.06 ms) or rate of desensitization (τ 3.0 ± 0.07 ms; n = 9) compared to control conditions (10–90% rise 0.52 ± 0.07 ms, τ 2.4 ± 0.02 ms, n = 11; p > 0.05, unpaired t-test). GluA1-S831A had the same response time course (10–90% rise 0.51 ± 0.07, τ 2.7 ± 0.03 ms; n = 10) as wild type receptors. CaMKII also enhanced the γ_{MEAN} of GluA1 receptors that included a mutation converting the PKA phosphorylation site Ser845 to alanine (n = 12–13 patches, data not shown). These results confirm that the primary effects of phosphorylation of GluA1-Ser831 are on single channel conductance[4]. We also observed a modest increase in open probability determined by non-stationary variance analysis when CaMKII was included in the patch pipette in cells co-transfected with wild-type GluA1 and a cDNA encoding the PKI inhibitor peptide [8] to reduce basal phosphorylation of Ser845.

Previous studies of the effects of CaMKII on recombinant AMPA receptors in the absence of TARPs showed that CaMKII can increase γ_{MEAN} in homomeric GluA1 but not GluA1/GluA2 heteromeric receptors[33]. We have replicated this result in homomeric GluA1

recombinant receptors carrying either a phosphodeficient or phosphomimic mutation at Ser831 (S831A and S831E, respectively). These GluA1 receptors also included a S845A mutation to prevent phosphorylation by endogenous PKA, as well as the L497Y[34] mutation to block macroscopically observed desensitization; we refer to GluA1-L497Y,S831A,S845A as GluA1-AA and GluA1-L497Y,S831E,S845A as GluA1-EA for simplicity. The γ_{MEAN} determined by variance analysis for GluA1-EA was significantly higher (γ_{MEAN} 14.2 ± 0.6 pS; n = 19) than GluA1-AA (γ_{MEAN} 9.4 ± 0.7 pS; n = 18; Table 1). Similar results were obtained for the double phosphomimic mutant GluA1-L497Y,S831D,S845D (γ_{MEAN} 13.1 ± 1.0 pS; n = 12; $p < 0.001$; Table 1). The open probability (P_O) of non-desensitizing receptors was unaffected by the phosphomimic mutations (Table 1). Consistent with previous findings[33], the GluA1 phosphomimic mutation does not increase γ_{MEAN} of heteromeric GluA1/GluA2 AMPA receptor responses recorded at −60 mV (Table 1); for all experiments, the edited version of GluA2- L483Y was used. Incorporation of edited GluA2 into the receptor complex lowered the conductance and yielded a linear IV curve (Table 1, Fig. 2a), confirming that responses were from heteromeric receptors. However, the γ_{MEAN} values were not significantly different between heteromeric receptors carrying the phosphodeficient GluA1-S831A mutation and the phosphomimic GluA1-S831E mutation ($p = 0.65$; Table 1). These results suggest that the effects of GluA1-Ser831 phosphorylation are determined by the AMPA receptor subunit composition.

HEK cells do not appear to express stargazin[35]. To examine the potential role of stargazin in CaMKII regulation of AMPA receptor function, we repeated experiments with homomeric and heteromeric receptors in cells co-expressing stargazin. As expected from previous studies, coexpression of stargazin increasedγ_{MEAN} of both homo- and heteromeric receptors (Table 1)[7, 36]. The presence of stargazin did not modify the effect of the phosphomimic mutation on homomeric GluA1 receptors (Table 1). The γ_{MEAN} of GluA1-EA mutant receptors in cells expressing stargazin (γ_{MEAN} 16.9 ± 1.0 pS; n = 8; Table 1) was significantly increased relative to phosphodeficient GluA1-AA receptors co-expressed with stargazin (γ_{MEAN} 12.3 ± 1.1 pS; n = 13; $p < 0.01$; Table 1). Importantly, the γ_{MEAN} of GluA1/GluA2 receptors containing the GluA1-EA phosphomimic mutation was significantly increased (γ_{MEAN} 6.2 ± 0.9 pS; n = 12; Table 1) compared to heteromeric receptors with the phosphodeficient GluA1-AA mutation in cells co-expressing stargazin (γ_{MEAN} 3.8 ± 0.4 pS; n = 10; $p < 0.05$; Table 1). That is, co-expression of stargazin with GluA1/GluA2 heteromeric receptors restored the effects of the GluA1-EA mutation on γ_{MEAN}. Open probability was not significantly altered by the phosphomimic mutation in all recordings from non-desensitizing receptors coexpressed with stargazin (Table 1). The overall conductance of GluA1/GluA2 receptors was lower than homomeric GluA1 receptors and was enhanced by co-expression of stargazin, confirming the interaction of stargazin and the presence of heteromeric GluA1/GluA2 receptors.

One potential confound of our interpretation is the possible presence of a subpopulation of homomeric GluA1-EA receptors in GluA1/GluA2/stargazin-transfected cells, which in theory could account for the observed conductance increase from the GluA1-S831E mutation. To determine whether the different conductance values for phosphomimic and phosphodeficient mutations might reflect a stargazin-enhanced subpopulation of homomeric GluA1 receptors, we repeated this experiment on outward currents recorded at a positive

holding potential. At +40 mV, the current contributed by GluA1 homomers should be negligible (Fig. 2a–b), allowing us to measure γ_{MEAN} for primarily heteromeric channels. At this holding potential, γ_{MEAN} of heteromeric receptors in the presence of stargazin was still increased by the GluA1-EA mutation (5.9 ± 0.6 pS) compared to GluA1-AA (2.9 ± 0.7 pS; $p < 0.01$). In homomeric GluA1 receptors, stargazin reduced the extent of inward rectification and reduced the rectification ratio of current recorded at +40 mV to −60 mV from 0.26 to 0.43. By contrast, the corresponding rectification ratio for cells expressing heteromeric GluA1/GluA2 (0.66) was not significantly changed upon co-expression of stargazin (Fig. 2a–b). From these values we calculate that 96% of the current recorded from GluA1/GluA2/stargazin transfected cells at +40 mV was from heteromeric receptors and 4% from homomeric receptors using the rectification ratios of homomeric GluA1 receptors (Methods). We used this relative contribution of GluA1 to the macroscopic current, the weighted γ_{MEAN} values we observed for homomeric receptors, and the weighted γ_{MEAN} for multiple subconductance levels described in equation 1 (Methods) to plot the γ_{MEAN} for mixture of phosphomimic and phosphodeficient GluA1 and GluA1/GluA2 receptors over a range of hypothetical GluA1/GluA2 conductance values (Fig. 2c). From this calculation, we can determine the maximal possible difference in the γ_{MEAN} caused solely by conductance contributed from homomeric receptors, underlying 4% of the macroscopic current (Fig. 2d). When the change in γ_{MEAN} caused by GluA1-EA is plotted over a range of hypothetical GluA1/GluA2 receptor γ_{MEAN} values, it is clear that the maximum possible conductance increase caused by the GluA1-S831E mutation cannot account for the 213% increase in γ_{MEAN} observed for GluA1/GluA2/stargazin receptors (Fig. 2d). These results support the finding that CaMKII phosphorylation of GluA1-Ser831 in AMPA receptors that contain the edited GluA2 subunit in complex with stargazin increases conductance.

While stargazin has been extensively studied, it is not the predominant TARP within the hippocampus. We therefore examined if phosphoSer831 increases the conductance of heteromeric AMPA receptors coexpressed with another TARP, γ8, which is highly expressed in the hippocampus, slows deactivation, slows desensitization, and prolongs the activation rise time of AMPA receptors[37–39]. Because the γ8 cDNA is in a vector that coexpresses GFP, expression of γ8 was confirmed via fluorescent imaging. The conductance of cells expressing GluA1-EA/GluA2/γ8 was increased to 6.4 ± 1.4 pS ($n = 10$) compared to 3.0 ± 0.4 pS in cells expressing GluA1-AA/GluA2/γ8 ($n = 11$; $p < 0.05$; student's t-test; Table 1). These data suggest that there is a common property between TARPs that, when in complex with GluA1-containing AMPA receptors, enables a phosphoSer831-dependent increase in conductance.

CaMKII increases channel conductance independent of efficacy

At the single channel level, AMPA receptors open to multiple discrete subconductance levels[23, 25–27]. Structural studies of the isolated agonist-binding domain have shown that it can adopt a range of ligand-dependent conformational states, and the extent of domain closure in these agonist-bound crystals is correlated with the probability that a subunit-associated gate will open[24, 26, 40]. Whereas the relationship between the degree of cleft closure observed in these structures and the extent and frequency of domain closure in full length receptors expressed in cells remains unclear[26], the single channel conductance

appears to be related to subunit-associated gating and agonist efficacy. This led us to hypothesize that Ser831 phosphorylation influences GluA1 subunit gating, which results in an increased relative frequency of larger conductance level openings. To test this hypothesis, we compared the effect of GluA1-Ser831 phosphorylation on recombinant homomeric GluA1 receptor responses to a range of structurally diverse partial agonists with varied efficacy. To confirm that GluA1-L497Y showed similar conductance levels as wild type GluA1, we evaluated single channel currents in outside out patches in response to a maximally effective concentration of glutamate. The average single channel subconductance levels from 9 patches containing GluA1-L497Y channels are similar to those previously described for wild type GluA1 receptors (Table 2)[8].

We analyzed the variance of macroscopic current responses from outside-out patches excised from cells transfected with GluA1-L497Y and activated by a variety of ligands (Fig. 3a–b). The agonists tested included glutamate and Cl-homoibotenic acid as representative agonists with high efficacy at GluA1, plus a set of 5-substituted willardiine analogues with low to medium efficacy relative to glutamate[26], [40], [41] (Fig. 3b). Variance analysis of the current responses (Fig. 3c) showed that conductance was correlated with relative agonist efficacy (Fig. 3d), as expected if agonists with lower efficacy have a decreased probability of activating an individual subunit[26]. Evaluation of the variance of the macroscopic response showed that inclusion of CaMKII in the pipette solution significantly increased γ_{MEAN} for all agonists when compared to patches with control solution in the pipette. The rank order of γ_{MEAN} produced by the various agonists was similar for both conditions (Supplemental Table S1).

CaMKII increases channel coupling efficiency

We have previously described the analysis of both variance and single channel recordings to quantify the coupling efficiency, ε, between agonist binding and gating for each subunit, which is defined as a value between 0 and 1[24], [26], [27]. The value ε describes the probability that an agonist-bound subunit will contribute to ion permeation, assuming all subunits function independently. The relative number of openings to the different conductance levels can be determined from the binomial probability of four subunits and their coupling efficiency (Methods). From these equations we can calculate the relationship between ε and γ_{MEAN} (Fig. 4a; Methods). From the theoretical relationship between γ_{MEAN} and ε for the conductance levels found for GluA1-L497Y homomeric AMPA receptors, the coupling efficiency of responses to each partial agonist can be extracted (Fig. 4b). By performing this analysis for responses with either control or CaMKII in the patch pipette, we can show that GluA1-Ser831 phosphorylation produces similar changes in ε regardless of agonist efficacy (Fig. 4c). These data strongly support our working hypothesis that phosphorylation of GluA1-Ser831 enhances the coupling efficiency between agonist binding and channel gating.

A correlation exists between the coupling efficiency and the degree of domain closure of the isolated GluA2 ligand binding domain bound to various agonists[26]. Although a comparable crystallographic data set does not exist for GluA1, we have used the degree of GluA2 domain closure as an estimate of GluA1 domain closure. CaMKII-induced changes in the

coupling efficiency occur independently of the degree of domain closure observed in structures of isolated agonist binding domains (Fig. 4d). We propose that the lack of correlation ($p = 0.09$) between domain closure and changes in coupling efficiency ($\Delta\varepsilon$) suggests that phosphorylation modifies the rate of the conformational changes required for channel activation independent of agonist binding, and the extent or frequency of ligand-induced domain closure. In other words, GluA1-Ser831 phosphorylation reduces the energy needed for a subunit to undergo transition to an active state that allows ion permeation

Ser831 controls single channel coupling efficiency

Previous studies have shown that HEK cells possess variable levels of endogenous PKA[8, 42] and PKC activity[43]. To eliminate the potentially confounding effects of variable levels of endogenous kinase and phosphatase activity, we utilized the phosphomutant receptors GluA1-S831A,S845A and GluA1-S831E,S845A to investigate whether CaMKII not only increases macroscopic but also the single channel coupling efficiency. Initially, we measured glutamate EC_{50} values for steady state responses in *Xenopus laevis* oocytes. Wild type glutamate EC_{50} was 16 ± 1 μM for wild type GluA1, 15 ± 1 μM for GluA1-S831A,S845A, and 11 ± 1 μM for GluA1-S831E,S845A ($p > 0.2$ by one-way ANOVA, n = 9–19). We subsequently performed single channel recordings from cell-attached membrane patches obtained from HEK cells expressing these same homomeric GluA1 mutant receptors. Although AMPA receptors possess a low single channel conductance, unitary channel currents were clearly identifiable in the presence of a maximally effective concentration of glutamate (2 mM; Fig. 5a–b). The profound desensitization of GluA1 receptors reduced the open probability and allowed discrete openings to be observed; individual channel openings occurred infrequently enough to suggest that simultaneous openings were rare. No channels were seen without glutamate added to the pipette or in untransfected cells. We subsequently fitted each opening to a filtered step response function of variable amplitude using the time course fitting method. Filtered step response functions were allowed to transition between open states or the closed state, allowing us to determine the number of conductance levels, amplitudes, and relative frequencies. Composite open time histograms constructed from all patches could be fitted with two exponential components. Fitted time constants and mean open times were similar between GluA1-S831A,S845A ($\tau1$ 0.33 ms, 58%; $\tau2$ 2.23 ms, 42%; mean open time 1.13 ms) and GluA1-S831E,S845A ($\tau1$ 0.37, 54%; $\tau2$ 1.63, 46%, mean open time 0.95 ms). Analysis of glutamate-activated GluA1 unitary currents in cell-attached patches from cells expressing either GluA1-S831A,S845A or GluA1-S831E,S845A yielded four subconductance levels of amplitudes that were similar to those of wild type GluA1 and GluA1-L497Y (Fig. 5a–b; Table 2). However, there was a shift to larger conductance levels in GluA1-S831E,S845A receptors compared to GluA1-S831A,S845A receptors (Fig. 5c–d; Table 3). That is, the relative proportion of openings to $\gamma2$ and $\gamma3$ doubled at the expense of $\gamma1$.

If we assume that these four subconductance levels reflect the opening of an AMPA channel when 1, 2, 3, or 4 of the agonist-bound subunits are activated (Fig. 5a), then the binomial theorem should predict the relative frequency of each sublevel for all possible values of subunit coupling efficiencies[26]. From the known values of the relative frequency and amplitude of openings to different conductance levels, we can determine ε from theγ_{MEAN}

that we measured using variance analysis. Single channel data in Table 2 reveals that ε is greater in homomeric GluA1 receptors expressing the mutation S831E than S831A (Fig. 5e). In addition, the binomial representation of subunit independent gating can account for the single channel properties in both GluA1-S831E,S845A and GluA1-S831A,S845A receptors (Fig. 5f). These data support the working hypothesis that phosphorylation of GluA1-Ser831 enhances subunit gating, which explains our findings, as well as previous work[4], showing that phosphoSer831 increases the frequency of larger conductance levels as individual subunits become more easily activated.

DISCUSSION

We have used macroscopic and single channel recording to explore the functional and structural mechanisms that underlie CaMKII-dependent regulation of GluA1-containing AMPA receptors. In addition, we have shown for the first time that CaMKII increases conductance of native hippocampal AMPA receptors specifically via actions at GluA1-Ser831, by evaluation of AMPA receptor response properties in the GluA1 phosphomutant knock-in mice. Moreover, previous studies in recombinant systems in the absence of TARPs established that CaMKII phosphorylation of GluA1-Ser831 increases the single channel conductance of homomeric GluA1 receptors, but not of heteromeric GluA1/GluA2 receptors[4], [33]. We have confirmed this result, but further show that the GluA1-S831E phosphomimic mutation increases conductance of heteromeric GluA1/GluA2 recombinant channels when either stargazin or γ8 are present. These observations suggest that the results and mechanisms described here are relevant to the large number of heteromeric GluA1/GluA2 receptors in neurons.

Two hypotheses exist to describe the mechanism underlying the change in conductance brought about by phosphoSer831. Either phosphorylation of GluA1-Ser831 increases ion flux through the pore for all conductance levels, or alters gating to allow larger conductance levels to open more often. Our data support the second hypothesis, since conductance level amplitudes of recombinant homomeric GluA1 receptors are unchanged by mimicking phosphorylation of Ser831. In a similar way, the TARP stargazin increases the frequency of larger GluA4 conductance level openings[7]. Moreover, our data show that phosphorylation of GluA1-Ser831 increases γ_{MEAN} for agonists of varying efficacy and subunit coupling efficiency independent of the degree of domain closure induced by these agonists, determined in crystal structures of the isolated ligand binding domain. This suggests that phosphorylation can facilitate the subunit-specific conformational changes that occur after agonist binding. This allows the pore to open to four quantized conductance levels related to the fraction of the four subunits that are activated at the moment the pore rapidly dilates. That is, our data are compatible with a model in which a conformational change that is independent of pore opening takes place in each of four agonist-bound subunits, and the conductance of the pore when open is set by the number of subunits that have undergone this conformational change. The position of the pre-M1 helix in the GluA2 structure[3] provides an interesting potential site at which agonist-induced rearrangement could influence pore conductance.

Our coupling efficiency calculations are based on the binomial expansion in which we make the assumption that the four subunits that comprise the AMPA receptor operate independently of one another. In light of the tetrameric GluA2 crystal structure which shows that the extracellular domains are likely arranged as a dimer-of-dimers[3], it is possible that all four subunits do not function independently. However, use of the binomial expansion to estimate coupling efficiency successfully describes single channel opening frequency for a variety of partial agonists at AMPA receptors[24, 26, 27]. Moreover, recent data suggest that detectable subunit cooperativity occurs at low but not high agonist concentrations[27]. Thus, if opposing subunits influence the function of one another, it seems likely that the effects on coupling efficiency are minimal for saturating concentrations of agonist used in this study.

Phosphorylation serves a critical role in the regulation of many facets of glutamate receptor function. PKA phosphorylates GluA1 to increase the peak response open probability, perhaps as a consequence of altering a slow equilibrium between functional and non-functional states, which may reflect binding and dissociation of intracellular proteins[8]. In addition, phosphorylation of GluA1 by PKC is critical for LTP expression and incorporation of GluA1 subunits into the synapse[44, 45]. Moreover, SAP97 and AKAP97 reduce the concentration of PKC necessary to phosphorylate GluA1-Ser831 by positioning it close to its substrate[46]. Regulation of GluA1 function and trafficking underlies many forms of activity-dependent synaptic plasticity[2, 6, 9, 10, 12, 13, 16, 19, 43, 47], and CaMKII-dependent phosphorylation of GluA1-Ser831 has been hypothesized to influence LTP and synaptic strength[10, 16]. Thus, understanding the functional and structural mechanisms of GluA1-Ser831 phosphorylation-induced changes in AMPA receptor function is crucial for understanding the molecular changes that occur during activity-dependent synaptic plasticity, a leading model of learning and memory. While this study establishes that GluA1-Ser831 phosphorylation enhances coupling efficiency independent of agonist efficacy, further studies are needed to establish the structural basis by which GluA1 phosphorylation changes AMPA receptor gating. One possible explanation is that intra- or inter-protein interactions may induce functional changes in the channel. Also, there are at least four GluA1 phosphorylation sites that are implicated in synaptic plasticity (Fig. 1a), including Ser818 (PKC)[44, 45], Ser831 (CaMKII, PKC)[4, 5, 17], Thr840 (PKC, p70S6 kinase)[48, 49], and Ser845 (PKA, cGMP-dependent protein kinase II)[8, 50]. The presence of four phosphorylation sites within only 27 residues of the GluA1 C-terminal domain raises intriguing structural, biophysical, and biological questions as to the function of this highly regulated region of the GluA1 protein. Functional interactions between these phosphorylation sites or between this region of GluA1 and potential intracellular interaction partners have yet to be experimentally addressed. Future work evaluating these ideas may provide a structural framework around which to further explore the mechanism by which GluA1 phosphorylation influences AMPA receptor function.

METHODS

Materials

Purified CaMKII and calmodulin were obtained from New England Biolabs (Ipswich, MA) and activated according to the manufacturer's protocol. NBQX (2,3-dihydroxy-6-nitro-7-

sulfamoyl-benzo[f]quinoxaline-2,3-dione, a non-selective AMPA receptor antagonist), and the AMPA receptor partial agonists (S)-(−)-5-fluorowillardiine (FW), (S)-(−)-5-iodowillardiine (IW), (S)-(−)-5-bromowillardiine (BW), (S)-willardiine (HW), (S)-CPW399 (CPW) and Cl-HIBO (CH), as well as DL-AP5 (NMDA receptor antagonist) and cyclothiazide (AMPA receptor desensitization blocker) were obtained from Tocris (Ellisville, MO). NS1209 was a gift from NeuroSearch A/S (Ballerup, Denmark). Spermine was obtained from Sigma-Aldrich (#S2876, St. Louis, MO). Poly-D-lysine was obtained from Millipore (#A-003-E). All cell biology reagents were from Gibco (Invitrogen, Carlsbad, CA) unless otherwise stated.

Molecular biology

The CMV-based mammalian expression vector pRK5 (BD Pharmingen, San Diego, CA) harbouring the coding sequences of the flip splice variants of the rat *GRIA1* and *GRIA2* genes (GeneBank, gi:6552333 and gi:204381) was used for transient expression of GluA1 and edited GluA2 in mammalian cells. The mutations GluA1-L497Y, GluA2-L483Y, as well as GluA1-Ser831, and GluA1-Ser845 mutations to alanine, glutamate, or aspartate were introduced by QuickChange mutagenesis (Stratagene, San Diego, CA). All mutations were verified by DNA sequencing (SeqWright, Fisher Scientific. Houston, TX). Stargazin was contained within a pCI-neo vector, γ8 was in an IRES-eGFP vector. GluA1 and GluA2 cDNA was provided by Peter Seeburg, and γ8 cDNA from Roger Nicoll.

Maintenance and transfection of HEK cells

Human embryonic kidney cells (HEK293; ATCC 1573, hereafter HEK cells) were grown in Dulbecco's modified Eagle's medium (Gibco #10569) supplemented with 10% (v/v) fetal calf serum (Gibco, #26400) and 1% penicillin-streptomycin (Gibco, #15140-122) in polystyrene culture dishes in a humidified atmosphere of 5% CO_2, 95% O_2, at 37°C. Growth media for transiently transfected GluA1 cells were supplemented with 100 μg/ml of NS1209 or 200 μM NBQX to protect transfected cells against excitotoxicity induced by endogenous glutamate in the growth media. Cells were dissociated using 0.05% trypsin-EDTA (Gibco, #25300), plated on 8 mm glass coverslips coated with 20 μg/ml poly-D-lysine contained in 24-well plate, and transfected 24 hours prior to experimentation using FuGENE6 (Invitrogen, Carlsbad, USA). Briefly, plasmid DNA was diluted in DMEM to 10 μg/ml, supplemented with 30 μl/ml FuGENE6, incubated for 15 min at 37° C, and added to cells using 20 μl mix per cm^2 growth area. Plasmid DNA harbouring a reporter cDNA encoding GFP (pMAXGFP, Amaxa Biosystems, Germany) was added to receptor DNA at a 1:4 ratio to identify transfected cells.

Preparation of hippocampal neuron cultures

All procedures involving the use of animals were reviewed and approved by the Emory University IACUC. The hippocampal formation was dissected from P0 wild-type C57Bl/6, GluA1-S831A, GluA1-S831A,S845A GluA1-S831D,S845D knock-in mice.[16] Tissue was incubated in medium comprised of (in mM): 82 Na_2SO_4, 30 K_2SO_4, 5.8 $MgCl_2$, 0.25 $CaCl_2$, 1 HEPES, 3.6% glucose, 0.1 kynurenic acid, phenol red, with pH adjusted to 7.4 with NaOH. Hippocampal tissue was digested in 20 μg/ml papain (#LS003124, Worthington

Biochemical, Lakewood, NJ) for 15 minutes then transferred to a 30 mg/ml ovomucoid trypsin inhibitor solution (Sigma-Aldrich, #T92531) for 15 minutes. The tissue was triturated in OPTI-MEM solution (Gibco, #31985) supplemented with 2.5% glucose using two Pasteur pipettes of different bore sizes. Cells were diluted to a concentration of 0.2 × 10^6 cells/ml in OPTI-MEM and 1 ml was plated onto 50 μg/ml poly-D-lysine-coated glass coverslips (diameter 8 mm) in 24 well plates. After settling for one hour, OPTI-MEM was exchanged for Neurobasal medium (Gibco, #21103), supplemented 1:500 v/v with 100X Glutamax (Gibco, #35050), 1:50 v/v with 50X B-27, and 1:100 v/v with 10,000 U/ml penicillin/streptomycin. Cells were cultured for 7 to 25 days in 95% O_2/5% CO_2 at 37°C and media was exchanged every 7 days.

Two electrode voltage clamp recording from Xenopus oocytes

Female *Xenopus laevis* were anesthetized using 0.3% ethyl 3-aminobenzoate (Sigma-Aldrich, #A5040), and the ovaries were surgically removed. Stage V and VI oocytes were isolated after a 2 hr incubation of the ovaries in 2 mg/ml collagenase at room temperature. Oocytes were injected the following day with 50 ng of cRNA encoding wild-type or mutant GluA1 that was transcribed *in vitro* (mMessage mMachine, Ambion). Injected oocytes were maintained at 17°C in Barth's solution containing gentamycin sulfate (0.1 mg/ml) for 3–6 d, after which recordings were made at 23°C from cells perfused in a solution containing (in mM) 115 NaCl, 5 HEPES, 2 KCl, 1.8 $CaCl_2$, pH 7.0 (23°C). Recording pipettes were filled with 3 M KCl. For measurements of potentiation of current responses by injection of CaMKII during recording, glutamate (1 mM) was used to activate steady-state current responses recorded during two-electrode voltage clamp before and 20 minutes after microinjection of 5–20 nl of purified CaMKII (20 ng/μl). The degree of potentiation was calculated as the ratio of the amplitude of the test response to the control response.

Voltage clamp recordings from outside-out patches

Outside-out membrane patches were excised from transiently-transfected HEK cells or cultured hippocampal neurons using thick-walled borosilicate micropipettes (1.5 mm OD, 0.86 mm ID, WPI, Sarasota FL) filled with internal solutions comprised of (in mM) 110 gluconic acid, 110 CsOH, 30 CsCl, 4 NaCl, 5 HEPES, 4.37 EGTA, 2.1 $CaCl_2$, 2.27 $MgCl_2$, 4 ATP, 0.3 GTP (23°C). The pH was adjusted to 7.3 with CsOH or NaOH. For some experiments the intracellular solution was supplemented with CaMKII and calmodulin. The free Ca^{2+} concentration (100 nM) was calculated using published stability constants for EGTA, and verified with the program Winmaxc. Spermine (100 μM) was included in the internal solution for all experiments on hippocampal neurons. Pipettes had a tip resistance of 4–8 MΩ. External recording solution for all experiments were comprised of (in mM) 150 NaCl, 10 HEPES, 3 KCl, 1 $CaCl_2$, 1 $MgCl_2$, pH 7.4; 310–330 mOsm. Currents were recorded (V_{HOLD} = −40 to −80 mV) with an Axopatch 200B amplifier (Molecular Devices, Union City, CA) or HEKA EPC9 amplifier (Lambrecht/Pfalz, Germany), filtered at 5 kHz (−3 dB), and digitized at 20 kHz. For measurement of non-desensitizing current responses, drugs dissolved in external recording solution were added to the excised patch by bath application. For measurement of rapidly desensitizing current responses, a piezobimorph-driven double-barrelled perfusion system was used to rapidly apply saturating concentrations of agonist onto excised membrane patches for 100–200 ms, as previously

described[42]. The time course of solution exchange across the laminar flow interface was estimated by liquid junction potential to be 0.2–0.4 ms (10–90% rise time); the time course of the junction potential change for our perfusion system was measured at the end of most experiments. Maximally effective concentrations of agonists (glutamate 1 mM; HW 200 μM; IW 100 μM; CPW 200 μM; BW 100 μM; CH 500 μM) were used based on previously determined EC_{50} values. For cultured neurons, NMDA receptor responses were blocked by the addition of 100 μM DL-AP5 and 1 mM Mg^{2+}. Internal pipette solutions that contained CaMKII and/or calmodulin were stored in a glass syringe on ice. Non-stationary and stationary variance analysis of macroscopic currents was carried out as previously described[8], [26], [29]. The weighted mean conductance is related to *j* subconductance levels by the equation:

$$\gamma_{MEAN} = \sum N\, p_j\, \gamma_j{}^2 / \sum N\, p_j\, \gamma_j \quad (1)$$

where *N* is the number of channels, γ_j is conductance of the j^{th} sublevel, and p_j is the open probability for each of the conductance levels. For determination of coupling efficiency ε, p_j was determined from binomial expansion for values of ε between 0 and 1. A theoretical curve relating coupling efficiency to weighted γ_{MEAN} was generated from equation 1 using measured conductance levels and the binomial equation (Fig 4). From this curve we estimated the relative sublevel occupancy for values of ε between 0 and 1 needed to obtain the expected weighted conductance. Coupling efficiency ε can then be determined by comparing this theoretical relationship to the experimental values for the weighted γ_{MEAN} from variance or single channel analysis of the GluA1 responses under various experimental conditions. The response amplitude to a maximally effective concentration of agonist can similarly be predicted from the probability of openings to each conductance level by

$$Response\ Amplitude = V \sum N\, p_j\, \gamma_j \quad (2)$$

where *V* is the membrane holding potential and *N*, γ, *p* are as defined above. Values of ε for different agonists can also be determined by comparison of the experimentally determined partial agonist/glutamate response amplitude ratio and the predicted relationship between ε and response ratio. Identical values of ε were determined using conductance or response amplitude (not shown).

Rectification ratios in Figure 2 were obtained from the equation

$$RR_{\text{observed}} = F_{A1}(RR_{A1\text{observed}}) + F_{A1A2}(RR_{A1A2\text{theory}}) \quad (3)$$

where F_{A1} is the fraction of the macroscopic current carried by homomeric GluA1, F_{A1A2} is the fraction of macroscopic current carried by heteromeric GluA1/GluA2, and $F_{A1} + F_{A1A2} = 1$. For GluA1/stargazin transfected cells $RR_{A1\text{observed}}$ was 0.43 and for GluA1/GluA2/stargazin transfected cells RR_{observed} was 0.66; a linear IV yields $RR_{A1A2\text{theory}}$ of 0.67. The predicted weighted γ_{MEAN} presented in Figure 2 was obtained by inserting expressions for macroscopic current where *N* is the number of channels and *P* is the open probability

$$F_{A1}=\frac{NP_{A1}(\gamma_{A1})}{NP_{A1}(\gamma_{A1})+NP_{A1A2}(\gamma_{A1A2})} \quad F_{A1A2}=\frac{NP_{A1A2}(\gamma_{A1A2})}{NP_{A1}(\gamma_{A1})+NP_{A1A2}(\gamma_{A1A2})} \quad (4,5)$$

into equation 1 (*Methods)*, yielding:

$$\gamma_{\mathrm{MEAN}}=F_{A1}\gamma_{A1}+F_{A1A2}\gamma_{A1A2} \quad (6)$$

Single-channel recordings from cell-attached patches

Recordings of single channel currents from HEK cells expressing recombinant GluA1 were made at room temperature using the cell-attached patch-clamp configuration with Sylgard-coated thick-walled micropipettes (1.5 mm OD, 0.86 mm ID) with resistances of 7–12 MΩ. The recording pipettes were filled with extracellular solution; holding potential was −80 to −100 mV (patch pipette +80 to +100 mV). The resting membrane potential (V_m) of each cell was measured under current clamp at the end of each experiment by disruption of the membrane. Single-channel activity was evoked by a maximally effective concentration of glutamate (2 mM) in the recording pipette. Recordswere digitized at 20 kHz and filtered on-line using a Gaussianfilter (5 kHz; −3 dB). Single-channel currents activated by glutamate are brief and of low amplitude and thus difficult to distinguish from momentary noise. To obtain an estimate of the relative amplitudes of subconductancestates, the following measures were taken to verify that analyzed signals were from glutamate-activated GluA1 channels. First, in 3 experiments in which 30 seconds of cell-attached current recordings were analyzed for single-channel openings in the absence of glutamate, the frequency of apparent transitions was on average 21-fold lower than the frequency of apparent transitions in the presence of 2 mM glutamate ($p < 0.001$). In addition, the mean unitary current amplitude in the absence of glutamate was 0.05 pA, lower than events detected in the presence of glutamate. This result strongly suggests that the unitary currents that we measured indeed arise from glutamate gating of homomeric GluA1 rather than patch breakdown or other sources of noise. Second, only patches with an R.M.S value <0.2 pA (after off-line filtering at 1 kHz −3 dB) for control records were included in analysis (mean R.M.S 0.12 ± 0.04 pA; *n* = 10 patches). Single-channel openings were analyzed using the time course fitting method implemented in SCAN (provided by D. Colquhoun, University College London, UK); transitions briefer than 2.0 × filter-risetimes (i.e. 98% of full amplitude) were excluded from the analysisof amplitude histograms. All apparent transitions greater in amplitude than 2 × R.M.S between the open and closed states were fitted, and the resulting idealized records were revised by imposition of a minimum resolvable duration for open and shut periods (120 μsec); refitting of the data imposing a 200 μsec resolution produced similar results. The data comprising the amplitude histograms were fitted to the sum of four Gaussian components by the maximum likelihood method using EKDIST (D. Colquhoun).

Statistical methods

Unless otherwise noted, results are expressed as mean ± SEM. Statistical analysis of pairwise or multiple comparisons were performed using ANOVA, or student’s t-test as appropriate. $p < 0.05$ was considered to be statistically significant.

Supplementary Material

Refer to Web version on PubMed Central for supplementary material.

Acknowledgments

This work was supported by the NIH (NS068464, NS036654 SFT), the Howard Hughes Medical Institute (RH), the Alfred Benzon Foundation (ASK, TGB) and the Lundbeck Foundation (AS). We thank Drs. Derkach and Howe for critical comments on the manuscript. The authors declare no competing interests.

References

1. Traynelis SF, et al. Glutamate receptor ion channels: structure, regulation, and function. Pharmacol Rev. 2010; 62:405–496. [PubMed: 20716669]
2. Malinow R, Malenka RC. AMPA receptor trafficking and synaptic plasticity. Annu Rev Neurosci. 2002; 25:103–126. [PubMed: 12052905]
3. Sobolevsky AI, Rosconi MP, Gouaux E. X-ray structure, symmetry and mechanism of an AMPA-subtype glutamate receptor. Nature. 2009; 462:745–756. [PubMed: 19946266]
4. Derkach V, Barria A, Soderling TR. Ca2+/calmodulin-kinase II enhances channel conductance of alpha-amino-3-hydroxy-5-methyl-4-isoxazolepropionate type glutamate receptors. Proc Natl Acad Sci U S A. 1999; 96:3269–3274. [PubMed: 10077673]
5. Barria A, Derkach V, Soderling T. Identification of the Ca2+/calmodulin-dependent protein kinase II regulatory phosphorylation site in the alpha-amino-3-hydroxyl-5-methyl-4-isoxazole-propionate-type glutamate receptor. J Biol Chem. 1997; 272:32727–32730. [PubMed: 9407043]
6. Shepherd JD, Huganir RL. The cell biology of synaptic plasticity: AMPA receptor trafficking. Annu Rev Cell Dev Biol. 2007; 23:613–643. [PubMed: 17506699]
7. Tomita S, et al. Stargazin modulates AMPA receptor gating and trafficking by distinct domains. Nature. 2005; 435:1052–1058. [PubMed: 15858532]
8. Banke TG, et al. Control of GluR1 AMPA receptor function by cAMP-dependent protein kinase. J Neurosci. 2000; 20:89–102. [PubMed: 10627585]
9. Holmes WR, Grover LM. Quantifying the magnitude of changes in synaptic level parameters with long-term potentiation. J Neurophysiol. 2006; 96:1478–1491. [PubMed: 16760350]
10. Benke TA, Luthi A, Isaac JT, Collingridge GL. Modulation of AMPA receptor unitary conductance by synaptic activity. Nature. 1998; 393:793–797. [PubMed: 9655394]
11. Malenka RC, Kauer JA, Zucker RS, Nicoll RA. Postsynaptic calcium is sufficient for potentiation of hippocampal synaptic transmission. Science. 1988; 242:81–84. [PubMed: 2845577]
12. Lee HK, et al. Phosphorylation of the AMPA receptor GluR1 subunit is required for synaptic plasticity and retention of spatial memory. Cell. 2003; 112:631–643. [PubMed: 12628184]
13. Lee HK, Barbarosie M, Kameyama K, Bear MF, Huganir RL. Regulation of distinct AMPA receptor phosphorylation sites during bidirectional synaptic plasticity. Nature. 2000; 405:955–959. [PubMed: 10879537]
14. Silva AJ, Stevens CF, Tonegawa S, Wang Y. Deficient hippocampal long-term potentiation in alpha-calcium-calmodulin kinase II mutant mice. Science. 1992; 257:201–206. [PubMed: 1378648]
15. Lamsa K, Irvine EE, Giese KP, Kullmann DM. NMDA receptor-dependent long-term potentiation in mouse hippocampal interneurons shows a unique dependence on Ca(2+)/calmodulin-dependent kinases. J Physiol. 2007; 584:885–894. [PubMed: 17884930]
16. Lee HK, Takamiya K, He K, Song L, Huganir RL. Specific roles of AMPA receptor subunit GluR1 (GluA1) phosphorylation sites in regulating synaptic plasticity in the CA1 region of hippocampus. J Neurophysiol. 2010; 103:479–489. [PubMed: 19906877]
17. Barria A, Muller D, Derkach V, Griffith LC, Soderling TR. Regulatory phosphorylation of AMPA-type glutamate receptors by CaM-KII during long-term potentiation. Science. 1997; 276:2042–2045. [PubMed: 9197267]

18. Mammen AL, Kameyama K, Roche KW, Huganir RL. Phosphorylation of the alpha-amino-3-hydroxy-5-methylisoxazole4-propionic acid receptor GluR1 subunit by calcium/calmodulin-dependent kinase II. J Biol Chem. 1997; 272:32528–32533. [PubMed: 9405465]
19. Hayashi Y, et al. Driving AMPA receptors into synapses by LTP and CaMKII: requirement for GluR1 and PDZ domain interaction. Science. 2000; 287:2262–2267. [PubMed: 10731148]
20. Luthi A, et al. Bi-directional modulation of AMPA receptor unitary conductance by synaptic activity. BMC Neurosci. 2004; 5:44. [PubMed: 15538948]
21. Poncer JC, Esteban JA, Malinow R. Multiple mechanisms for the potentiation of AMPA receptor-mediated transmission by alpha-Ca2+/calmodulin-dependent protein kinase II. J Neurosci. 2002; 22:4406–4411. [PubMed: 12040047]
22. Palmer MJ, Isaac JT, Collingridge GL. Multiple, developmentally regulated expression mechanisms of long-term potentiation at CA1 synapses. J Neurosci. 2004; 24:4903–4911. [PubMed: 15163681]
23. Smith TC, Howe JR. Concentration-dependent substate behavior of native AMPA receptors. Nat Neurosci. 2000; 3:992–997. [PubMed: 11017171]
24. Poon K, Nowak LM, Oswald RE. Characterizing single-channel behavior of GluA3 receptors. Biophys J. 2010; 99:1437–1446. [PubMed: 20816055]
25. Rosenmund C, Stern-Bach Y, Stevens CF. The tetrameric structure of a glutamate receptor channel. Science. 1998; 280:1596–1599. [PubMed: 9616121]
26. Jin R, Banke TG, Mayer ML, Traynelis SF, Gouaux E. Structural basis for partial agonist action at ionotropic glutamate receptors. Nat Neurosci. 2003; 6:803–810. [PubMed: 12872125]
27. Prieto ML, Wollmuth LP. Gating modes in AMPA receptors. J Neurosci. 2010; 30:4449–4459. [PubMed: 20335481]
28. Wenthold RJ, Petralia RS, Blahos J II, Niedzielski AS. Evidence for multiple AMPA receptor complexes in hippocampal CA1/CA2 neurons. J Neurosci. 1996; 16:1982–1989. [PubMed: 8604042]
29. Traynelis SF, Jaramillo F. Getting the most out of noise in the central nervous system. Trends Neurosci. 1998; 21:137–145. [PubMed: 9554720]
30. Derkach VA. Silence analysis of AMPA receptor mutated at the CaM-kinase II phosphorylation site. Biophys J. 2003; 84:1701–1708. [PubMed: 12609872]
31. Swanson GT, Kamboj SK, Cull-Candy SG. Single-channel properties of recombinant AMPA receptors depend on RNA editing, splice variation, and subunit composition. J Neurosci. 1997; 17:58–69. [PubMed: 8987736]
32. Tomita S, Stein V, Stocker TJ, Nicoll RA, Bredt DS. Bidirectional synaptic plasticity regulated by phosphorylation of stargazin-like TARPs. Neuron. 2005; 45:269–277. [PubMed: 15664178]
33. Oh MC, Derkach VA. Dominant role of the GluR2 subunit in regulation of AMPA receptors by CaMKII. Nat Neurosci. 2005; 8:853–854. [PubMed: 15924137]
34. Stern-Bach Y, Russo S, Neuman M, Rosenmund C. A point mutation in the glutamate binding site blocks desensitization of AMPA receptors. Neuron. 1998; 21:907–918. [PubMed: 9808475]
35. Deng F, Price MG, Davis CF, Mori M, Burgess DL. Stargazin and other transmembrane AMPA receptor regulating proteins interact with synaptic scaffolding protein MAGI-2 in brain. J Neurosci. 2006; 26:7875–7884. [PubMed: 16870733]
36. Soto D, Coombs ID, Kelly L, Farrant M, Cull-Candy SG. Stargazin attenuates intracellular polyamine block of calcium-permeable AMPA receptors. Nat Neurosci. 2007; 10:1260–1267. [PubMed: 17873873]
37. Milstein AD, Nicoll RA. TARP modulation of synaptic AMPA receptor trafficking and gating depends on multiple intracellular domains. Proc Natl Acad Sci U S A. 2009; 106:11348–11351. [PubMed: 19549880]
38. Milstein AD, Zhou W, Karimzadegan S, Bredt DS, Nicoll RA. TARP subtypes differentially and dose-dependently control synaptic AMPA receptor gating. Neuron. 2007; 55:905–918. [PubMed: 17880894]
39. Nicoll RA, Tomita S, Bredt DS. Auxiliary subunits assist AMPA-type glutamate receptors. Science. 2006; 311:1253–1256. [PubMed: 16513974]

40. Hogner A, et al. Structural basis for AMPA receptor activation and ligand selectivity: crystal structures of five agonist complexes with the GluR2 ligand-binding core. J Mol Biol. 2002; 322:93–109. [PubMed: 12215417]
41. Frandsen A, et al. Tyr702 is an important determinant of agonist binding and domain closure of the ligand-binding core of GluR2. Mol Pharmacol. 2005; 67:703–713. [PubMed: 15591246]
42. Traynelis SF, Wahl P. Control of rat GluR6 glutamate receptor open probability by protein kinase A and calcineurin. J Physiol. 1997; 503 (Pt 3):513–531. [PubMed: 9379408]
43. Roche KW, O'Brien RJ, Mammen AL, Bernhardt J, Huganir RL. Characterization of multiple phosphorylation sites on the AMPA receptor GluR1 subunit. Neuron. 1996; 16:1179–1188. [PubMed: 8663994]
44. Boehm J, et al. Synaptic incorporation of AMPA receptors during LTP is controlled by a PKC phosphorylation site on GluR1. Neuron. 2006; 51:213–225. [PubMed: 16846856]
45. Lin DT, et al. Regulation of AMPA receptor extrasynaptic insertion by 4.1N, phosphorylation and palmitoylation. Nat Neurosci. 2009; 12:879–887. [PubMed: 19503082]
46. Tavalin SJ. AKAP79 selectively enhances protein kinase C regulation of GluR1 at a Ca2+-calmodulin-dependent protein kinase II/protein kinase C site. J Biol Chem. 2008; 283:11445–11452. [PubMed: 18305116]
47. Lisman J, Raghavachari S. A unified model of the presynaptic and postsynaptic changes during LTP at CA1 synapses. Sci STKE. 2006; 2006:re11. [PubMed: 17033044]
48. Lee HK, et al. Identification and characterization of a novel phosphorylation site on the GluR1 subunit of AMPA receptors. Mol Cell Neurosci. 2007; 36:86–94. [PubMed: 17689977]
49. Delgado JY, et al. NMDA receptor activation dephosphorylates AMPA receptor glutamate receptor 1 subunits at threonine 840. J Neurosci. 2007; 27:13210–13221. [PubMed: 18045915]
50. Serulle Y, et al. A GluR1-cGKII interaction regulates AMPA receptor trafficking. Neuron. 2007; 56:670–688. [PubMed: 18031684]

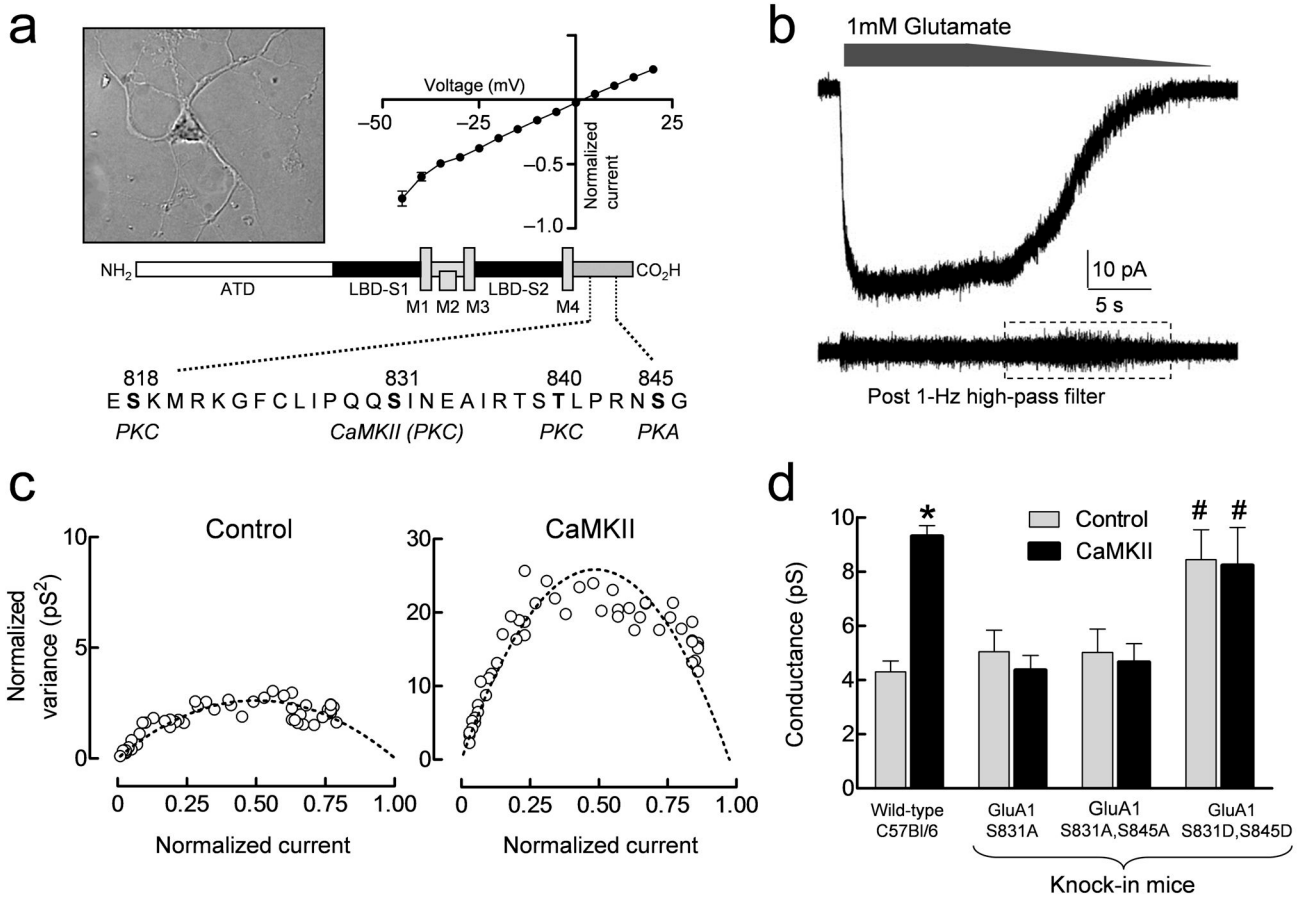

Figure 1.

CaMKII enhances γ_{MEAN} of hippocampal AMPA receptors recorded in outside-out patches from cultured hippocampal neurons. **A.** Photomicrograph of cultured hippocampal neurons with current-voltage relationship and a schematic representation of the AMPA receptor C-terminal domain (CTD) highlighting the four known serine/threonine phosphorylation sites (residues highlighted in black). **B.** Representative macroscopic current response to 1 mM glutamate in excised outside-out patches with 100 μM DL-AP5 and 1 mM Mg^{2+} present to block NMDA receptors and cyclothiazide to block AMPA receptor desensitization. The lower trace shows the response after high pass filtering, illustrating the increase in membrane current noise (dashed box) during channel deactivation. **C.** Representative normalized current-variance relationships are shown for two patches to allow comparison of the effects of γ_{MEAN} (see Methods) for GluA1 responses with and without CaMKII in the pipette. **D.** Summary of CaMKII effects on γ_{MEAN} of native AMPA receptors in cultured hippocampal neurons from either wild-type or knock-in mutant mice (mean ± SEM). * $p < 0.001$ for CaMKII compared to control in wild type neurons by t-test. # $p < 0.001$ compared to GluA1-S831A,S845A and GluA1-S831A by two-way ANOVA with Bonferroni's post hoc test. Data are from 8–15 neurons for each condition.

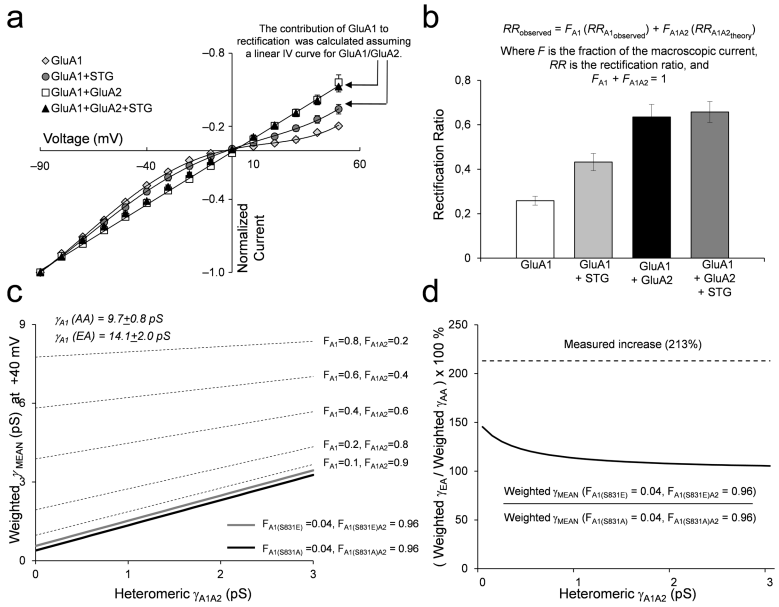

Figure 2.

The increase in γ_{MEAN} from GluA1/GluA2/stargazin transfected cells in is not caused by a stargazin-induced increase in a subpopulation of homomeric GluA1 receptors. **A.** Normalized current-voltage relationship for GluA1±stargazin and GluA1/GluA2±stargazin (mean ± SEM). **B.** Rectification ratios (RR) were calculated as the ratio of current amplitude at +40 mV, which reflects primarily GluA1/GluA2 heteromeric receptor current, to that at −60 mV (mean ± SEM; n = 8–18 cells for each condition). From the stargazin-induced change in the rectification ratio, we estimate that co-transfection with GluA1, GluA2, and stargazin leads to 96% GluA1/GluA2 receptors and 4% homomeric GluA1 (Methods). **C.** The predicted weighted mean conductance is plotted as a function of an unknown GluA1/GluA2 conductance according to equations 4–6 (see Methods). The broken lines show how the weighted γ_{MEAN} changes with progressively increasing F_{A1} using the conductance of GluA1-S831A and GluA1-S831A/GluA2. The thick black line is the weighted γ_{MEAN} when F_{A1} is the 4% of homomeric GluA1-S831A receptors with γ_{MEAN} of 9.7 pS determined at +40 mV, and 96% GluA1-S831A/GluA2. The thick gray line shows weighted γ_{MEAN} for GluA1-S831E with γ of 14.1pS determined at +40 mV and 96% GluA1-S831E/GluA2. **D.** The relationship between the change in weighted γ_{MEAN} induced by the GluA1-S831E alone in a mixed population of GluA1 (4%) and GluA1/GluA2 (96%) receptors over a range of GluA1/GluA2 conductance values. The dotted line shows that the experimentally observed γ_{MEAN} is more than that predicted from a conductance increase in only the GluA1 subpopulation.

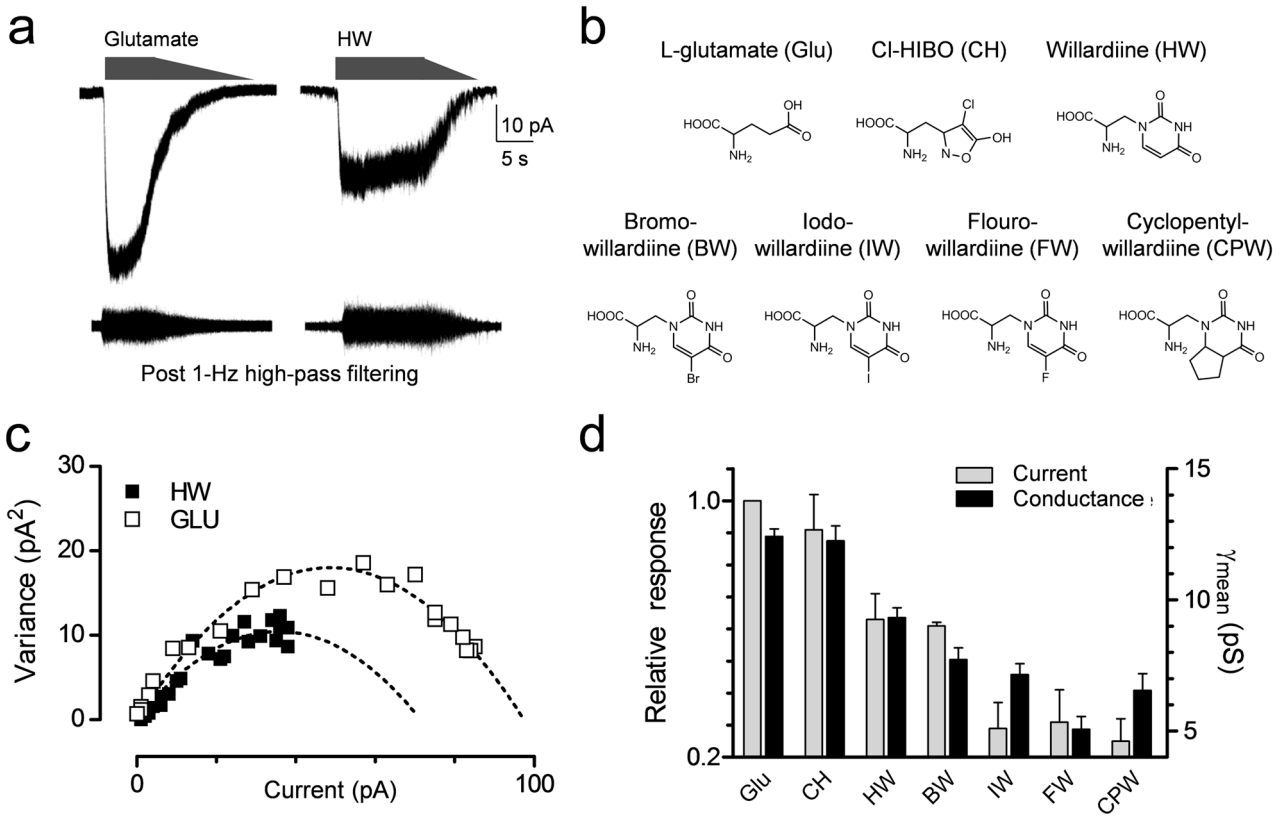

Figure 3.

Phosphorylation of GluA1-Ser831 changes γ_{MEAN} independent of agonist efficacy**. A.** Example of macroscopic currents and isolated difference currents for glutamate and willardiine activation of recombinant GluA1-L497Y in the same patch from HEK cells. **B.** Structures of the agonists used. **C.** The current-variance relationships are superimposed for glutamate and willardiine. **D.** There is a correlation (R = 0.95, p = 0.001) between the maximal response induced by agonists (expressed as a ratio to current induced by maximally effective glutamate) and the γ_{MEAN} obtained from variance analysis. Data are from 5–22 patches for each agonist.

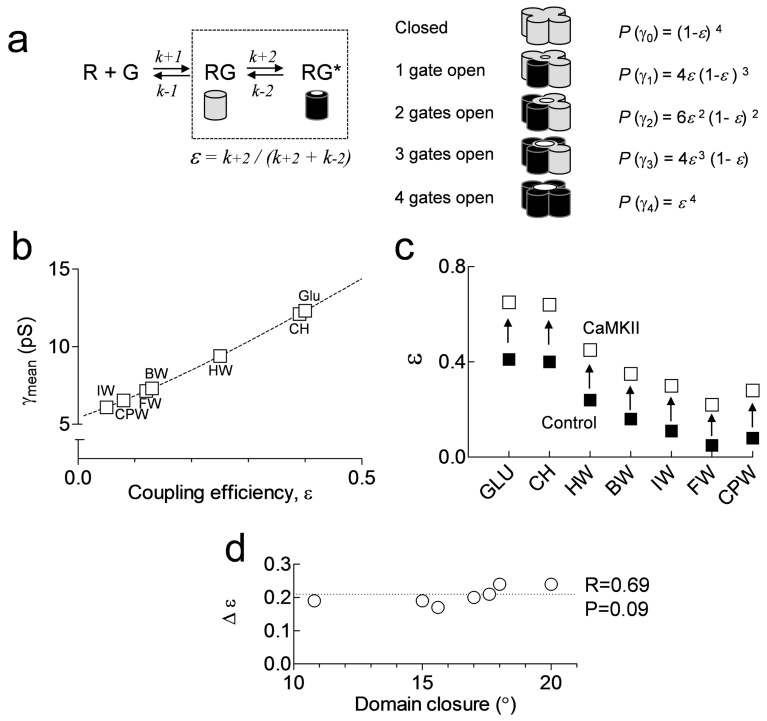

Figure 4.

GluA1-Ser831 phosphorylation increases the coupling efficiency between agonist binding and gating. **A.** AMPA receptor subunits contribute to gating once each subunit binds glutamate and becomes activated (RG*). The efficiency with which each subunit couples to gating (ε) can be calculated from rates of activation as shown. We assume that the distribution of channel conductance levels (γ) reflects binomial statistics, which allows calculation of the probability of each conductance level, or *P*(γ). **B.** The relationship between coupling efficiency and weighted mean conductance for data from partial agonists activating recombinant GluA1 receptors expressed in HEK cells. The dotted line shows the relationship between γ_{MEAN} and ε for the conductance levels found for GluA1-L497Y using a variety of agonists (see Methods). **C.** Summary of the effects of CaMKII on coupling efficiency ε for each partial agonist. **D.** Relationship between agonist-induced domain closure of the GluA2 ligand binding domain[26, 41] and the change in GluA1 coupling efficiency (Δε). The degree of domain closure for Br-HIBO was used for Cl-HIBO[40]. The change in GluA1 coupling efficiency by CaMKII is not correlated (R = 0.69) with domain closure ($p > 0.05$).

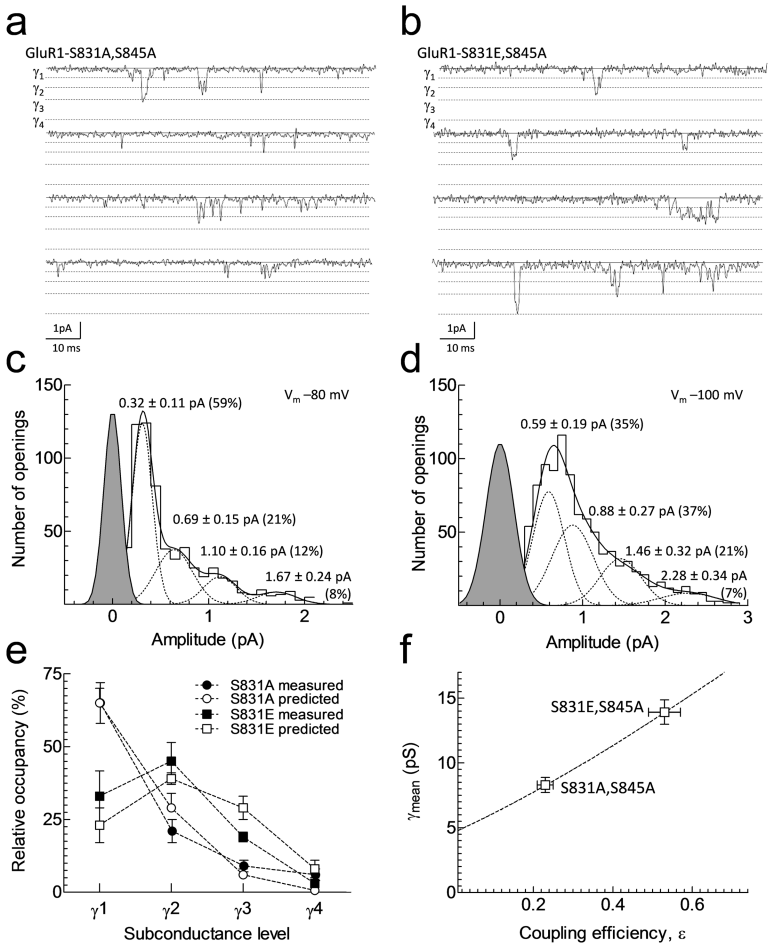

Figure 5.

GluA1-S831E phosphomimic mutation increases the frequency of higher conductance level openings and increases the single channel coupling efficiency. **A,B.** Individual single channel current traces recorded from recombinant phosphomutant GluA1-S831A,S845A and GluA1-S831E,S845A in cell-attached membrane patches in HEK cells with 2 mM glutamate in the patch pipette. These receptors were desensitizing and did not contain the L497Y mutation. **C,D.** Representative amplitude histogram from individual patches constructed from the fitted amplitudes of individual openings using time course fitting. Histograms were fitted with the sum of four Gaussian components (± STD). **E.** The binomial theory correctly predicts the relative proportion of subconductance levels for GluA1-S831A and GluA1-S831E mutations given the calculated values for coupling efficiency for GluA1 in cyclothiazide in Table 3. **F.** The relationship between coupling efficiency and mean conductance was constructed similar to Fig. 4b using values for γ_{MEAN} listed in Table 3 for GluA1 in cyclothiazide; error bars are SEM. The dotted line shows the relationship between γ_{MEAN} and ε constructed similar to Fig. 4b.

Table 1

Effect of CaMKII and GluA1-Ser831 phosphomimic and phosphodeficient mutations on weighted mean unitary conductance (γ_{MEAN}) of homomeric and heteromeric GluA1-containing receptors expressed in HEK cells. Some cells were co-transfected with a cDNA encoding the PKI inhibitor peptide[9]

	Mutation	TARPs	Method	γ_{MEAN}	P_O	N
GluA1/PKI	WT	--	Non-stationary	12.0 ± 1.0	0.53 ± 0.08	9
GluA1/PKI + CaMKII	WT	--	Non-stationary	20.4 ± 2.9 *	0.74 ± 0.03 *	11
GluA1/PKI	S831A	--	Non-stationary	12.9 ± 1.2	0.35 ± 0.06	8
GluA1/PKI + CaMKII	S831A	--	Non-stationary	11.1 ± 1.7	0.36 ± 0.05	10
GluA1	L497Y	--	Stationary	12.4 ± 0.3	0.77 ± 0.02	19
GluA1 + CaMKII	L497Y	--	Stationary	17.6 ± 0.4 *	0.76 ± 0.02	22
GluA1	L497Y, S831A, S845A	--	Stationary	9.4 ± 0.7	0.79 ± 0.03	18
GluA1	L497Y, S831E, S845A	--	Stationary	14.2 ± 0.6 **	0.73 ± 0.03	19
GluA1	L497Y, S831D, S845D	--	Stationary	13.1 ± 1.0 **	0.75 ± 0.02	12
GluA1	L497Y, S831A, S845A	Stargazin	Stationary	12.3 ± 1.1	0.96 ± 0.03 **	13
GluA1	L497Y, S831E, S845A	Stargazin	Stationary	16.9 ± 1.0 **	0.95 ± 0.02 **	8
GluA1/GluA2	L497Y, S831A, S845A	--	Stationary	2.6 ± 0.5	0.78 ± 0.03	8
GluA1/GluA2	L497Y, S831E, S845A	--	Stationary	3.0 ± 0.2	0.82 ± 0.02	11
GluA1/GluA2	L497Y, S831A, S845A	Stargazin	Stationary	3.8 ± 0.4	0.71 ± 0.02	10
GluA1/GluA2	L497Y, S831E, S845A	Stargazin	Stationary	6.2 ± 0.9 ***	0.79 ± 0.05	12
GluA1/GluA2	L497Y, S831A, S845A	γ8	Stationary	3.0 ± 0.4	0.68 ± 0.07	10
GluA1/GluA2	L497Y, S831E, S845A	γ8	Stationary	6.4 ± 1.4 ***	0.78 ± 0.07	11

Weighted mean unitary conductance, γ_{MEAN}, was determined using either non-stationary or stationary variance analysis of current responses obtained from transfected HEK cells. Values are mean ± SEM; N is the number of outside-out patches studied at a holding potential of −60 mV.

* $p < 0.05$ significantly different from control (recordings lacking CaMKII); there was no significant difference between GluA1-S831A, GluA1-S831A + CaMKII or WT GluA1 control (ANOVA).

** $p < 0.01$ significantly different from GluA1-L497Y,S831A,S845A, GluA1-L497Y,S831E,S845A or from GluA1-L497Y,S831A,S845A + stargazin (One-way ANOVA, with Tukey's post hoc test). Coexpression with stargazin is described in the *Methods*.

*** $p < 0.05$ significantly different from heteromeric receptors containing GluA1-L497Y,S831A,S845A mutant subunits (One-way ANOVA, with Tukey's post hoc test). Open probability (P_O) was calculated as the ratio of the maximal macroscopic current to the product of the fitted unitary current and number of channels. One-way ANOVA was used to compare P_O values for homomeric GluA1 L497Y mutant and GluA1/GluA2 receptor responses.

Table 2

Single channel conductance levels and their relative distribution in wild-type and mutant homomeric GluA1 receptors expressed in HEK cells

	γ_1		γ_2		γ_3		γ_4		N
	pS	**(%)**	**pS**	**(%)**	**pS**	**(%)**	**pS**	**(%)**	
Wild-type GluA1[a]	4 ± 1	-	8 ± 1	-	15 ± 1	-	25 ± 1	-	
GluA1-L497Y	5 ± 1	21 ± 4	10 ± 1	37 ± 5	17 ± 1	35 ± 4	23 ± 1	7 ± 2	**9**
GluA1-S831A,S845A	4 ± 1	64 ± 3	9 ± 1	21 ± 2	15 ± 1	9 ± 1	21 ± 2	6 ± 1	**5**
GluA1-S831E,S845A	5 ± 1	31 ± 6	9 ± 1	45 ± 5	14 ± 1	19 ± 1	25 ± 2	5 ± 1	**5**
Average	*5*		*9*		*15*		*24*		

GluA1-L497Y values were determined from outside-out patches. GluA1-S831A,S845A and GluA1-S831E,S845A values were determined from cell-attached patches. All values are mean ± SEM.

[a] Wild type GluA1 values from[8].

Table 3

Effect of Ser831 phosphomutations on recombinant homomeric GluA1 receptor coupling efficiency, ε

	γ_{MEAN} (pS)	ε	γ_{MEAN} (pS)	ε	Δε	N
	Control		CaMKII			
GluA1[a]	12.0 ± 1.0	0.45	20.4 ± 2.9	0.84	0.39	9, 11
GluA1-L497Y[b]	12.4 ± 0.3	0.47	17.6 ± 0.4	0.71	0.24	19, 22
	S831A,S845A		S831E,S845A			
GluA1[b,c]	8.3 ± 0.6	0.24	13.9 ± 0.9	0.54	0.30	23, 11
GluA1- L497Y[b]	9.4 ± 0.7	0.29	14.2 ± 0.6	0.54	0.25	18, 19

Homomeric GluA1 macroscopic current responses in outside-out patches from HEK cells were induced by 1 mM glutamate followed by a slow washout. Variance analysis of the response was used to estimate weighted mean conductance (γ_{MEAN}). Values are mean ± SEM.

[a] Non-stationary variance analysis from Table 1

[b] Stationary variance analysis

[c] Currents recorded in the presence of 100 μM cyclothiazide